



Electrochemical insights into the inhibitory efficiency of crude leaf extract of *Datura discolor* against corrosion of low-carbon steel in low pH media – EIS and PDP Approaches

Cornelius C. Ahanotu ^{a,c,*}, Veronica O. Ezigbo ^b, Sylvia I. Okonkwo ^b

^a Department of Science Laboratory Technology, Imo State Polytechnic, Omuma, P.M.B 1472, Owerri, Nigeria

^b Department of Pure and Industrial Chemistry, Chukwuemeka Odumegwu Ojukwu University, P.M.B 02, Uli, Anambra State, Nigeria

^c Department of Chemical Sciences, Claretian University of Nigeria, Nekede, P.M.B 1019, Owerri, Nigeria

*Corresponding author, Email address: cornelahanotu@gmail.com

Received 01 Feb 2023,

Revised 20 Feb 2024,

Accepted 21 Feb 2024

Keywords:

- ✓ *Datura discolor*;
- ✓ Corrosion inhibitor;
- ✓ Angel's trumpet;
- ✓ Devil thorn-apple;
- ✓ Adsorption

Citation:

Ahanotu C.C., Ezigbo V.O. & Okonkwo S.I. (2024). Electrochemical insights into the inhibitory efficiency of crude leaf extract of *Datura discolor* against corrosion of low-carbon steel in low pH media – EIS and PDP approaches. *J. Mater. Environ. Sci.*, 15(2), 251-267

Abstract: Methanol leaf extract of *Datura discolor* Bernh (DD) was investigated for its anticorrosion effect on low-carbon steel corroding in 0.5 M solutions of H₂SO₄, HCl and HNO₃ by using electrochemical impedance spectroscopy (EIS) and potentiodynamic polarization (PDP) techniques. Three inhibitor packages were prepared by extracting the DD leaves using the respective acid solutions (0.5 M solutions of H₂SO₄, HCl and HNO₃) as solvent following the procedure of hot extraction under reflux for 2 hours at room temperature. Open circuit potential (OCP) was first measured against elapsed time of immersion of coupons and recorded for the three systems for 30 min using 150 ml of the test acid solution. DD leaf extract was found to retard the corrosion of low-carbon steel in the hostile acidic environments by the adsorbed film of organic molecules interacting at the substrate-acid solution interface. Inhibitor efficiency ($\eta\%$) was found to be a function of both extract (inhibitor) concentration and corrosive medium. With 150 mg/L of extract, inhibitor efficiency ($\eta\%$) of >77 % in H₂SO₄, >60 % in HCl, and >35 % in HNO₃ were recorded via electrochemical impedance spectroscopy, while >75 % in H₂SO₄, >65 % in HCl, and >34 % in HNO₃ were recorded via potentiodynamic polarization measurements. These results are quite consistent and indicate that the inhibitor exhibited the best efficacy in sulfuric acid medium and the least efficacy in nitric acid. The impedance responses in the three acidic media suggests that the corrosion reaction occurred under charge transfer control. Values of the corrosion potential (E_{corr}) did not change significantly. The maximum change in corrosion potential recorded in all the experiments is < 85 mV and this suggests that DDL-extract functioned as a mixed-type inhibitor. The results of this study affirms that *Datura discolor* leaf extract could be harnessed as a sustainable inhibitor for protecting low-carbon steel from acid-induced corrosion.

1. Introduction

Metals and alloy metals such as steel corrode when they react with another substance such as oxygen, hydrogen, an electric current or even dirt and bacteria. Generally, corrosion occurs when most or all of the atoms of the same metal surface are oxidized, damaging the entire surface (Eddy & Ebenso, 2008). Most metals are easily oxidized, *i.e.* they tend to lose electrons to oxygen (and other substances) in the air or in water. As oxygen is reduced by gain electrons, it forms an oxide with the metal.

The dissolution of iron and steel surfaces *via* acid attack during acid cleaning, descaling and pickling can normally be controlled by introduction of appropriate corrosion inhibiting additives, to hinder or suppress the corrosion reaction and suppress the corrosion reaction (Khadom *et al.*, 2015; El Ouafi *et al.*, 2002; Mihi *et al.*, 2006). Some organic compounds are known to be potent as corrosion inhibitors for different grades of steel in acidic and alkaline media (Dafali *et al.*, 2002; Oguzie *et al.*, 2005; Oguzie, 2005; Mihit *et al.* 2006; Oguzie, 2006). Other research scholars (Satapathy *et al.*, 2009; da Rocha *et al.*, 2010) have also reported that many materials of plant origin have been successfully used to reduce metal corrosion in the past. The extracts from seeds, barks, leaves, and root of these plant materials contain an array of natural products and have been tested for their corrosion inhibitory properties and some have been reported to successfully inhibit metal corrosion in acidic media (Ebenso *et al.*, 2008; Raja *et al.*, 2008; Abboud *et al.*, 2009; Okafor *et al.*, 2010; Hmamou *et al.*, 2012 & 2015).

Natural products from plant materials are gaining global popularity and acceptance as a source of pharmacological and therapeutic agents not only in traditional medicine and as excellent drug candidates for drug discovery and development, as dyes in textile industries, insecticides in agriculture, but also as inhibitors of corrosion of metal and alloys in the field of material science (Diass *et al.*, 2023; Haddou *et al.*, 2023; Wang *et al.*, 2023; Ahanotu *et al.*, 2022, Ahanotu *et al.*, 2020; Kasiri & Safapour, 2014; Oguzie *et al.*, 2007). As corrosion of different grades of steel in the chemical, petroleum and petrochemical industries continues to be a serious menace, material scientists have tried to make use of organic inhibitors of plant origin which have been affirmed globally to be cheap, ecofriendly, non-toxic and biodegradable unlike inorganic and synthetic inhibitors. This work employed the methanol leaf extract of *Datura discolor* (angel's trumpet or desert thorn-apple) as a promising inhibitor to clamp down the menace of corrosion using low-carbon steel as experimental specimen. No scientific information is currently available about *Datura discolor* as regards its corrosion inhibitory effect. *Datura discolor* Bernh., commonly known as angel's trumpet (or desert thorn-apple) is a herbaceous annual plant native to Sonoran Desert of western North America. The plant belongs to the family, *Solanaceae* which contains over 3,000 species distributed among more than 90 genera around the world. Some of these genera are genus *Datura* (e.g. angel's trumpet which is *Datura discolor*), genus *Solanum* (e.g. eggplant, tomato, potato), genus *Nicotiana* (e.g. tobacco), as well as genus *Capsicum* (e.g. *Capsicum annuum*). This study therefore seeks to investigate the corrosion inhibitory effect of crude extract of the leaves of *Datura discolor* using electrochemical techniques, with a view to determining its efficacy and sustainability as inhibitor for preserving low-carbon steel from acid attack. The photos of *Datura discolor* are shown in Figure 1.

2. Experimental Methodology

2.1 Collection of leaf sample and procurement of carbon steel specimens

Fresh and healthy leaves of *Datura discolor* Bernh. were plucked from the live plant at Ifakala Town in Mbaitoli Local Government Area of Imo State, Nigeria. Identity of the plant was validated by a Plant Scientist after which the leaves were thoroughly washed, sun-dried to constant weight for 14 days, ground to fine powdered form and preserved in an amber coloured container prior to use. Low-carbon steel sheets were procured from the Materials and Metallurgical Engineering Workshop of the Federal University of Technology, Owerri, Imo State, Nigeria. The sheets were mechanically cut into test coupons of specific dimensions (30 mm long \times 20 mm wide \times 1.5 mm thick) and a cylindrical hole of 3.0 mm diameter was drilled in each coupon using a lathe machine. The low-carbon steel is of the same grade and chemical composition with Fe as the chief element (99.048% w/w) as reported elsewhere (Puspitasari *et al.*, 2017).



Plate A



Plate B

Figure 1. Photos of *Datura discolor* showing the leaves and fruits

2.2 Extraction

The finely ground leaves of *Datura discolor* was subjected to extraction by maceration using methanol and after filtration, solvent was completely removed by evaporation to dryness using a water bath and a slurry extract was obtained. The respective acid corrodent solutions (0.5 M solutions of H₂SO₄, HCl, and HNO₃) were used in turns as solvents to prepare the inhibitor test solutions.

2.3 Electrochemical determinations

To achieve system stability, open circuit potential (OCP) was first measured against elapsed time and recorded for the three systems for 1800 s (30 mins) using 150 ml of the test acid solution and in accordance to standard procedures (Ahanotu *et al.*, 2020). This is necessary in order for the substrate (carbon steel coupon) to dissolve at its equilibrium potential and avoid charging current and these are the conditions required of a stable OCP. Thereafter, all the electrochemical experiments were carried out at the stable OCP condition. The electrochemical tests were carried out using an electrochemical workstation (Metrohm autolab, PGSTAT204 potentiostat), which is a cell assembly consisting of three electrodes namely; 1 cm² exposed low carbon steel surface which served as the working electrode (WE), silver/silver chloride (Ag/AgCl) which served as a reference electrode (RE), and a platinum wire which was deployed as a counter electrode (CE). All the reported potentials in this work are with respect to Ag/AgCl, The electrolytes for the current investigation are 0.5 M solutions of H₂SO₄, HCl, and HNO₃ which were utilized in the extraction of the DDL-inhibitor molecules and also served as the corrosive media both in the absence and presence of various concentrations of the inhibitor (*Datura discolor* leaf extract). The electrochemical impedance spectroscopy (EIS) was measured with a signal amplitude perturbation of 10 mV throughout a frequency range of 100 kHz–10 mHz. The potentiodynamic polarization investigation was conducted at the potential range of ± 250 mV versus OCP at scanning rate of 0.2 mV s⁻¹. The experimental data were later analyzed using appropriate electrochemical analytical softwares such as Zsimpwin 3.2 model and EC-lab for EIS and potentiodynamic polarization, respectively.

3. Results and Discussion

3.1 OCP studies

Figure 2 shows the plots of open circuit potential (OCP) versus time for the corrosion reaction in the three acidic environments (H_2SO_4 , HCl and HNO_3) for 30 minutes stabilization time and represented as potential (V vs. Ag/AgCl) versus immersion time.

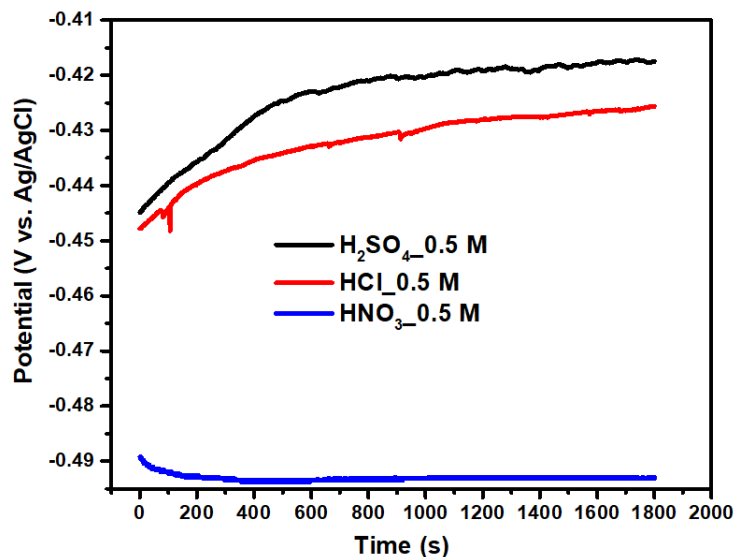


Figure 2. Variation of open circuit potential (OCP) with elapsed time for low-carbon steel corroding in H_2SO_4 , HCl and HNO_3 systems at room temperature

The plotted data are recorded as the change in potential difference between the working electrodes (the corroding low carbon coupons) and the reference electrode with respect to time when immersed in the electrolytes (the hostile acidic corrodents). The working electrode is Ag/AgCl. The data were recorded at the starting point of the electrochemical experiments. The figure shows that the OCP is stable for the three corrosive environments, indicating that the corroding coupons have reached steady state and the experiments may begin.

3.2 Findings from electrochemical experiments using 0.5 M H_2SO_4 solution

The data from electrochemical impedance spectroscopy and potentiodynamic polarization evaluated for low carbon steel/electrolyte interface without and with different concentrations of DDL-based inhibitor in 0.5 M H_2SO_4 solution at room temperature are shown as spectra in Figure 3.

Figure 3, panels a, b and c indicate the electrochemical impedance data presented as impedance spectra which, respectively, represent the Nyquist impedance plots, Bode plots and Phase-angle plots recorded for low carbon steel corroding in 0.5 M H_2SO_4 solution without and with different concentrations of DDL-based inhibitor. Nyquist plots obtained at every concentration followed similar pattern and transcends into the shape of semicircles having depressed centre along the x -axis. It is observed in Figure 3a that adding 150 mg/L of DDL-based inhibitor produces an increase in the diameter (or size) of the depressed semicircles relative to that of the blank (uninhibited) environment, with a corresponding increase in impedance of the interface in Figure 3b, and also in the maximum phase-angle in Figure 3c. These trends suggest the suppression of the corrosion reaction (dissolution of the test specimens). This phenomenon is commonly associated with metal-electrolyte interaction occasioned by the roughness and heterogeneity of the electrode surface (Fawcett *et al.*, 1992; Solomon *et al.*, 2010).

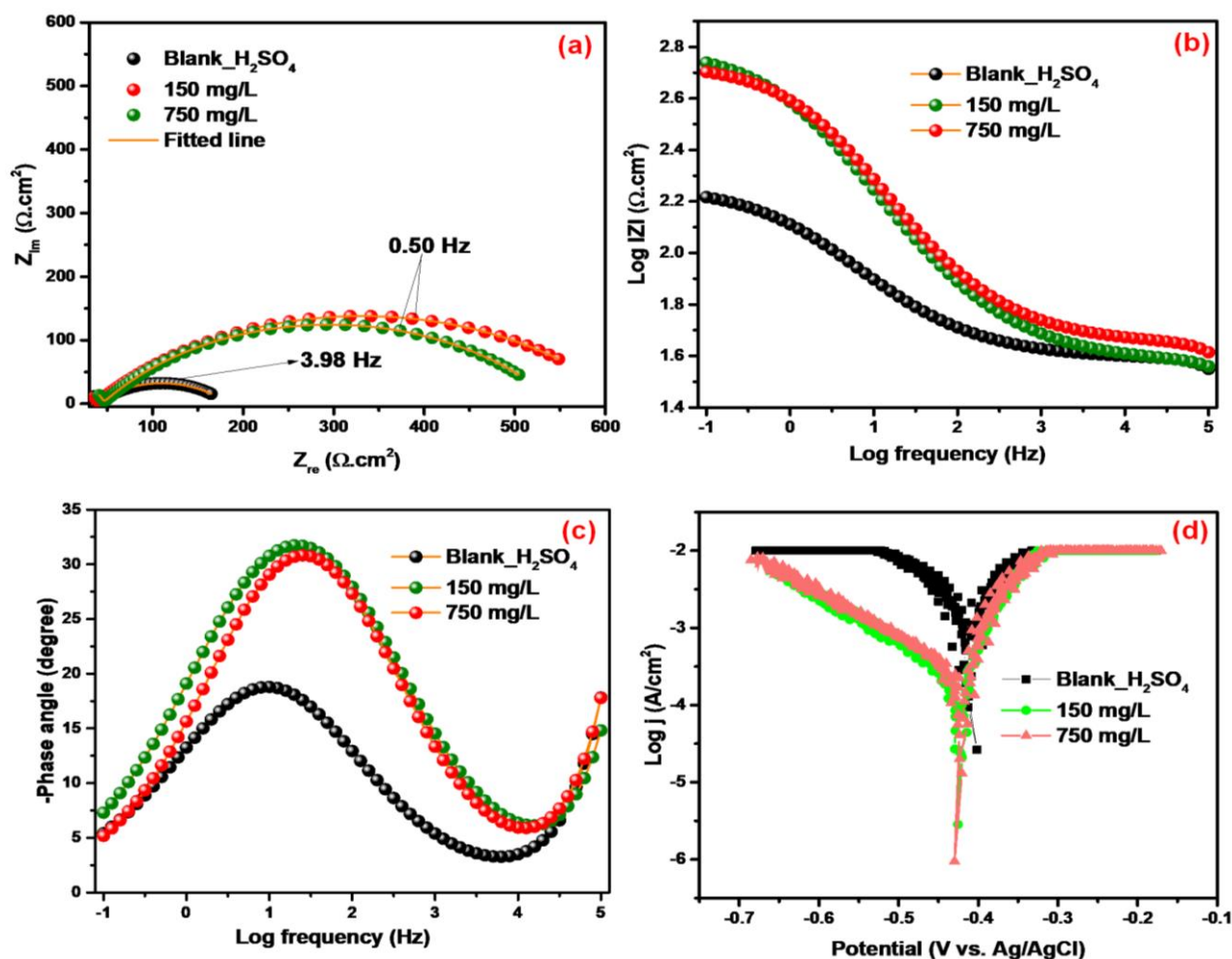


Figure 3. Electrochemical impedance spectra and potentiodynamic polarization curves for low carbon steel in 0.5 M H₂SO₄ at room temperature; (a) Nyquist impedance plots (b) Bode plots (c) Phase-angle plots, and (d) Tafel anodic and cathodic polarization curves

The electrochemical impedance spectrum for the Nyquist plots were fitted to an equivalent circuit model (ECM) shown in Figure 4 to help interpret the corrosion inhibition process. A similar circuit has been previously adopted in modeling mild steel/electrolyte interface as described elsewhere (Oguzie *et al.*, 2007). The equivalent circuit in Figure 4 consists of a solution resistance (R_s) which is shorted by a parallel arrangement of the polarization resistance (R_{po}) and constant phase element 1 (CPE_1), which is in turn shorted by another parallel arrangement of charge transfer resistance (R_{ct}) and constant phase element 2 (CPE_2). The constant phase elements (CPE_1 and CPE_2) are equivalent electrical circuit components that model the behavior of an electric double-layer, that is to say that they are impact capacitors and their capacitance is referred to as the double-layer capacitance (C_{dl}). The polarization resistance (R_{po}) is the resistance impacted by the adsorbed inhibitor layer against water penetration, while the charge transfer resistance (R_{ct}) is a measure of electron transfer across the specimen-solution interface and is inversely proportional to the corrosion rate (Al-Moghrabi *et al.*, 2019).

The value of the charge transfer resistance indicates transfer of electrons across the specimen/solution interface. The use of the constant phase elements has been reported previously in literature (Larabi *et al.*, 2005; Popova *et al.*, 2003) and is deployed in the model to compensate for the inhomogeneity in the electrode as depicted in the depressed nature of the Nyquist semicircle. The impedance (Z) of the

constant phase elements is a function of the surface factor (n), magnitude of CPE (Q) which is a constant, and angular frequency (ω) used for the study and is deduced using Equation 1 as previously reported (Larabi *et al.*, 2005; Popova *et al.*, 2003).

$$Z_{CPE} = Q^{-1}(j\omega)^{-n} \quad (1)$$

where $j = (-1)^{1/2}$ represents an imaginary number, and ω is the angular frequency in $rad\ s^{-1}$ ($\omega = 2\pi f$, where f is the frequency in Hz). The frequency at which the imaginary component of the impedance is a maximum ($-Z''_{max}$) is given by Equation 2 according to a report by Kissi *et al.* (2006).

$$f(-Z''_{max}) = \frac{1}{2\pi C_{dl} R_{ct}} \quad (2)$$

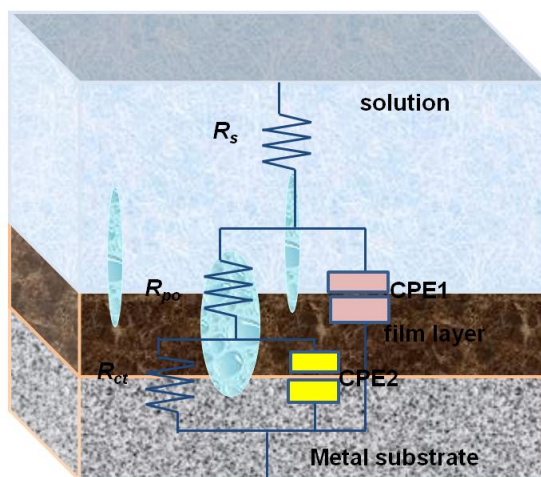


Figure 4. Electrochemical equivalent circuit used for all EIS model fit

Introduction of the inhibitor alters the surface property of the electrode (test coupon) and it can be effectively monitored by assessing the change in values of double-layer capacitance (C_{dl}) at the carbon steel-acid solution interface. The value of double-layer capacitance (C_{dl}) at different concentrations were calculated using Equation 3 as previously employed by Umoren *et al.* (2011).

$$C_{dl} = (Y_0 \cdot R_{ct}^{1-n})^{1/n} \quad (3)$$

It is a common knowledge that inhibitors clamp down the corrosion of metals and alloys by getting adsorbed on the substrate surface, forming a thin film or layer which consequently affects the double-layer capacitance (C_{dl}). The C_{dl} can be deduced using the following expression;

$$C_{dl} = \varepsilon^0 \varepsilon \frac{A}{t} \quad (4)$$

where ε is dielectric constant of medium, ε^0 is dielectric constant of space, A is the surface area of the electrode and t is thickness of the adsorbed inhibitor layer or film formed at the substrate-electrolyte interface. The values of the electrochemical fitting parameters deduced from the Nyquist plots are given in Table 1.

From the data, it is evident that the corrosion process occurred under charge transfer control. Addition of 150 mg/L DDL-based inhibitor into the hostile acid corrodent resulted to an increase in the charge transfer resistance from 143.5 to 647.04 $\Omega \cdot cm^{-2}$, accompanied by a depreciation in the magnitude of CPE_1 from 1.27 to 0.98 $\Omega^{-1} cm^{-2}$ (determinant of the double-layer capacitance). The depreciation

of the CPE_1 connotes a decrease in the double-layer capacitance (C_{dl}). This trend could be attributed to the adsorption of the DDL-based inhibitor on the carbon steel-electrolyte interface which consequently increases the thickness of the electrical double layer and/or decreases the dielectric constant with an increase in concentration of the inhibitor (Al-Moghrabi *et al.*, 2019; Oguzie *et al.*, 2007; Sayed *et al.*, 2003; Kissi *et al.*, 2006; Larabi *et al.*, 2005; Popova *et al.*, 2003). This translates to a corresponding decline in the corrosion rate of the low-carbon steel specimen with an increase in the inhibitor concentration and this is brought about by the adsorption of the inhibitor molecules onto the substrate/electrolyte interface, thereby preserving the test substrate from acid attack.

Table 1. EIS fitting data for corrosion of low carbon steel in 0.5 M H₂SO₄ solution without and with different concentrations of DDL-based inhibitor extract at room temperature

C_{inh} (mg/L)	R_s ($\Omega \cdot cm^2$)	CPE_1		R_{po} ($\Omega \cdot cm^2$)	CPE_2		R_{ct} ($\Omega \cdot cm^2$)	X^2 (10^{-1})	η_{EIS} (%)
		$Y_{01}(x10^{-8})$ ($\Omega^{-1} cm^{-2}$)	n_1		$Y_{02}(x10^{-8})$ ($\Omega^{-1} cm^{-2}$)	n_2			
Blank	0.01	1.27	0.80	32.08 ± 0.11	0.17	0.90	143.50 ± 0.12	1.30	-
150	0.01	0.98	0.91	37.96 ± 0.44	0.45	0.97	647.04 ± 0.32	1.01	77.82
750	0.02	1.06	0.86	33.88 ± 0.34	0.35	0.98	496.12 ± 0.12	1.02	71.08

It is a general belief that the parameter n known as the surface factor is a measure of the electrode surface heterogeneity (roughness), and its increase in the inhibited environment relative to the blank (uninhibited) environment suggests a decrease in surface roughness of the test coupons resulting from the adsorption of the added inhibitor molecules on the substrate surface and increased thickness of protective film at the substrate-acid interface. This leads to a decline in corrosion rate of the test coupon in the acid electrolyte.

The inhibitor efficiency ($\eta\%$) of 77.82 % was produced upon addition of 150 mg/L of DDL-based inhibitor as observed from Table 1. This is in agreement with the trend established in the mass loss experiments. It can also be seen that the values of the polarization resistance (R_{po}) and charge transfer resistance (R_{ct}) are directly proportional to the concentration of the DDL-extract. The R_{po} increased from $32.08 \Omega \cdot cm^2$ in the uninhibited environment (blank) to $37.96 \Omega \cdot cm^2$ upon addition of 150 mg/L of DDL-extract, while R_{ct} increased from $143.50 \Omega \cdot cm^2$ to $647.04 \Omega \cdot cm^2$, with a corresponding increase in inhibitor efficiency relative to the blank medium. The values of the inhibitor efficiency were estimated by comparing the value of charge transfer resistance in the blank (uninhibited) environment, $R_{ct(b)}$ and that of the protected (inhibited) environment, $R_{ct(inh)}$ using Equation 5 as according to Oguzie *et al.* (2007):

$$\eta\% = \frac{R_{ct(inh)} - R_{ct(b)}}{R_{ct(inh)}} \times 100 \quad (5)$$

The slight drop in the inhibitor efficiency in the second inhibited environment containing 750 mg/L could be due to a condition in which the substrate surface has reached saturation point with the adsorbed inhibitor layer. At this point, the inhibition process was characterized by an initial increase in the degree of surface coverage with increasing inhibitor dosage until a particular concentration was reached beyond which the increase in the degree of surface coverage with extract concentration became limited (Eddy *et al.*, 2010; Al-Mhyawi, 2014; Ihebrodike *et al.*, 2010; Li *et al.*, 2019; Ofuyekpone *et al.*, 2021). The inhibitor concentration at such a saturation point is known as inhibitor optimum

concentration. A similar trend has been reported by other research scholars (Deng & Li, 2012; Hossain *et al.*, 2022). It is, therefore, evident that 750 mg/L exceeded the optimum concentration of the inhibitor needed for the saturation of the coupon surfaces. Hence, the inhibitor efficiency gradually depreciated due to desorption of the inhibitor molecules on the carbon steel surface. Figure 3d shows the Tafel polarization curves for the anodic and cathodic potentials of low carbon steel in the hostile environment after 30 min of immersion in 0.5 M H₂SO₄ solution without and with different concentrations of DDL-based inhibitor at temperature. The electrochemical parameters obtained from the potentiodynamic polarization measurements such as the corrosion potential (E_{corr}), the corrosion current density (I_{corr}), the anodic (β_a) and cathodic (β_c) Tafel slopes, the inhibitor efficiency ($\eta\%$) and the degree of surface coverage (θ) after the stabilization time are calculated from the polarization curves of carbon steel coupons and summarized in Table 2.

Table 2. Potentiodynamic (Tafel) polarization parameters recorded for low carbon steel corroding in 0.5 M H₂SO₄ at room temperature

C_{inh} (mg/L)	E_{corr} (mV vs. Ag/AgCl)	I_{corr} (mA cm ⁻²)	β_a (mV dec ⁻¹)	β_c (mV dec ⁻¹)	$\eta\%$	θ
Blank	-380.57 ± 2.11	899.06 ± 1.11	160.12	88.11	-	-
150	-430.57 ± 1.08	221.75 ± 1.02	76.30	98.43	75.34	0.75
750	-430.61 ± 1.07	271.49 ± 0.18	68.81	66.31	69.80	0.69

A cursory look at Figure 3d shows that the corrosion potential was shifted towards the cathodic (passive) region upon addition of the inhibitor. The polarization curves seem to be parallel in the cathodic region which is evident in shape of the cathodic Tafel curves. Conversely, the change in the anodic Tafel curves are very noticeable. This suggests that reduction reaction at the cathode (evolution of hydrogen gas) was not much influenced by increasing inhibitor concentration, and that inhibitory effect resulted to reduced rate of dissolution of the coupons in the acid. This trend is similar to what Ji *et al.* (2013) has earlier reported. Ofuyekpone *et al.* (2021) has earlier reported that a corrosion inhibitor is a mixed-type inhibitor if the recorded change in corrosion potential is < 85 mV while values of corrosion potential >85 mV suggests either anodic or cathodic type inhibitor. The highest shift (change) in the corrosion potential recorded in this experiment was 50.04 mV, hence a mixed-type behavior was indicated. The data in Table 2 show that the corrosion current density is markedly reduced from 899.06 mA cm⁻² in the blank environment to 221.75 mA cm⁻² upon addition of 150 mg/L of the DDL-extract, signifying declining corrosion rate since current is associated with the flow of electrons. The reduced corrosion rate accounted for an inhibitor efficiency of 75.34 % relative to the blank environment. This reduction in corrosion current density (or corrosion rate) is likely due to the formation of a protective layer on the carbon steel surface which restricts the charge transfer reactions, and consequently further dissolution of the steel in the electrolyte (Palumbo *et al.*, 2023). This is in agreement with the trend established in the mass loss experiments. The inhibitor efficiency was calculated from the polarization data according to Oguzie *et al.* (2007) using the expression in Equation 6.

$$\eta\% = \frac{I_{corr} - I_{corr(inh)}}{I_{corr}} \times 100 \quad (6)$$

where I_{corr} and $I_{corr(inh)}$ are respectively the corrosion current density without and with the DDL-based inhibitor. It is observed that $\eta\%$ values deduced are concordant with those deduced from the electrochemical impedance measurements.

It is evident from the data that, as the concentration of the inhibitor is increased, the corrosion potential did not change significantly in the inhibited environments and the anodic Tafel constant maintained a steady decrease. This indicates that the DDL-based inhibitor has a pronounced corrosion inhibitory impact on the coupons in H₂SO₄ medium. The slight drop in the inhibitor efficiency observed in the Nyquist plots fitting data in Table 1 plays out here, revealing a depreciation of the inhibitor efficiency from 75.34 % to 69.80 %. This is also an indication that the optimum concentration of the DDL-based inhibitor necessary for the saturation of the working electrode surface (low-carbon steel surface) was exceeded when 750 mg/L of the extract was added in the second inhibited environment (Eddy *et al.*, 2010; Al-Mhyawi, 2014; Ihebrodike *et al.*, 2010; Li *et al.*, 2019; Deng & Li, 2012; Hossain *et al.*, 2022). Again, the values of the anodic Tafel constant are more strongly changed than the cathodic Tafel constant in the presence of the DDL-based inhibitor and corrosion potential did not change in the presence of the inhibitor. This suggests that anodic mode of inhibitory action of the DDL-based extract is more pronounced than that of the cathodic polarization. The results of both mass loss and polarization approaches revealed that the DDL-based offers a very good protection to the test specimens against corrosion in sulfuric acid medium.

3.3 Findings from electrochemical experiments using 0.5 M HCl Solution

The data from electrochemical impedance spectroscopy and potentiodynamic polarization evaluated for low carbon steel/electrolyte interface without and with different concentrations of DDL-based inhibitor in 0.5 M HCl solution at room temperature are shown as spectra in Figure 5.

Figure 5, panels a, b and c indicate the electrochemical impedance data presented as impedance spectra which, respectively, represent the Nyquist impedance plots, Bode plots and Phase-angle plots recorded for low carbon steel corroding in 0.5 M HCl solution without and with different concentrations of DDL-based inhibitor. After 1800 s of free immersion in the 0.5 M HCl solution without and with the inhibitor, it could be observed that the low-carbon steel attained a stable open circuit potential as revealed in Figure 4. The Nyquist plots (Figure 5a) obtained at every extract concentration again displayed identical shapes that are of different sizes, the diameters increasing as a function of extract dosage. The addition of inhibitor enlarges the Nyquist semicircles maximally at 150 mg/L of the extract, producing protection efficiency of 60.78 % relative to the blank or uninhibited environment. This was accompanied with a corresponding increase in impedance of the interface as seen in the Bode plots in Figure 5b, and also in the maximum phase-angle in Figure 5c. This enlargement of the Nyquist semicircles underscores the improved corrosion resistance impacted on the low-carbon steel coupons by the DDL extract, a phenomenon which is commonly associated with metal-electrolyte interaction caused by the roughness and inhomogeneity of the electrode surface (Fawcett *et al.*, 1992; Solomon *et al.*, 2010; Lebrini *et al.*, 2007). The values of the electrochemical fitting parameters deduced from the Nyquist plots are given in Table 3. It can also be seen that the values of the polarization resistance (R_{po}) and charge transfer resistance (R_{ct}) are directly proportional to the concentration of the DDL-extract. The R_{po} increased from 25.82 $\Omega \cdot cm^2$ in the uninhibited environment (blank) to 26.32 $\Omega \cdot cm^2$ upon addition of 150 mg/L of DDL-extract, while R_{ct} increased from 264.20 $\Omega \cdot cm^2$ to 673.68 $\Omega \cdot cm^2$, with a corresponding increase in inhibitor efficiency relative to the blank medium. The inhibitor efficiency was calculated from the experimental data according to Oguzie *et al.* (2007) using the expression in Equation 5. The value of CPE_I was also found to decrease with increasing inhibitor concentration. This trend suggests that the adsorption of the DDL-based inhibitor on the carbon steel-electrolyte interface consequently increases the thickness of the electrical double layer and/or decreases the dielectric constant with an increase in concentration of the inhibitor

(Al-Moghrabi *et al.*, 2019; Oguzie *et al.*, 2007; Sayed *et al.*, 2003; Kissi *et al.*, 2006; Larabi *et al.*, 2005; Popova *et al.*, 2003). The fitting of the electrochemical impedance spectrum for the Nyquist plots to an equivalent circuit model (ECM) is the same as that shown in Figure 4.

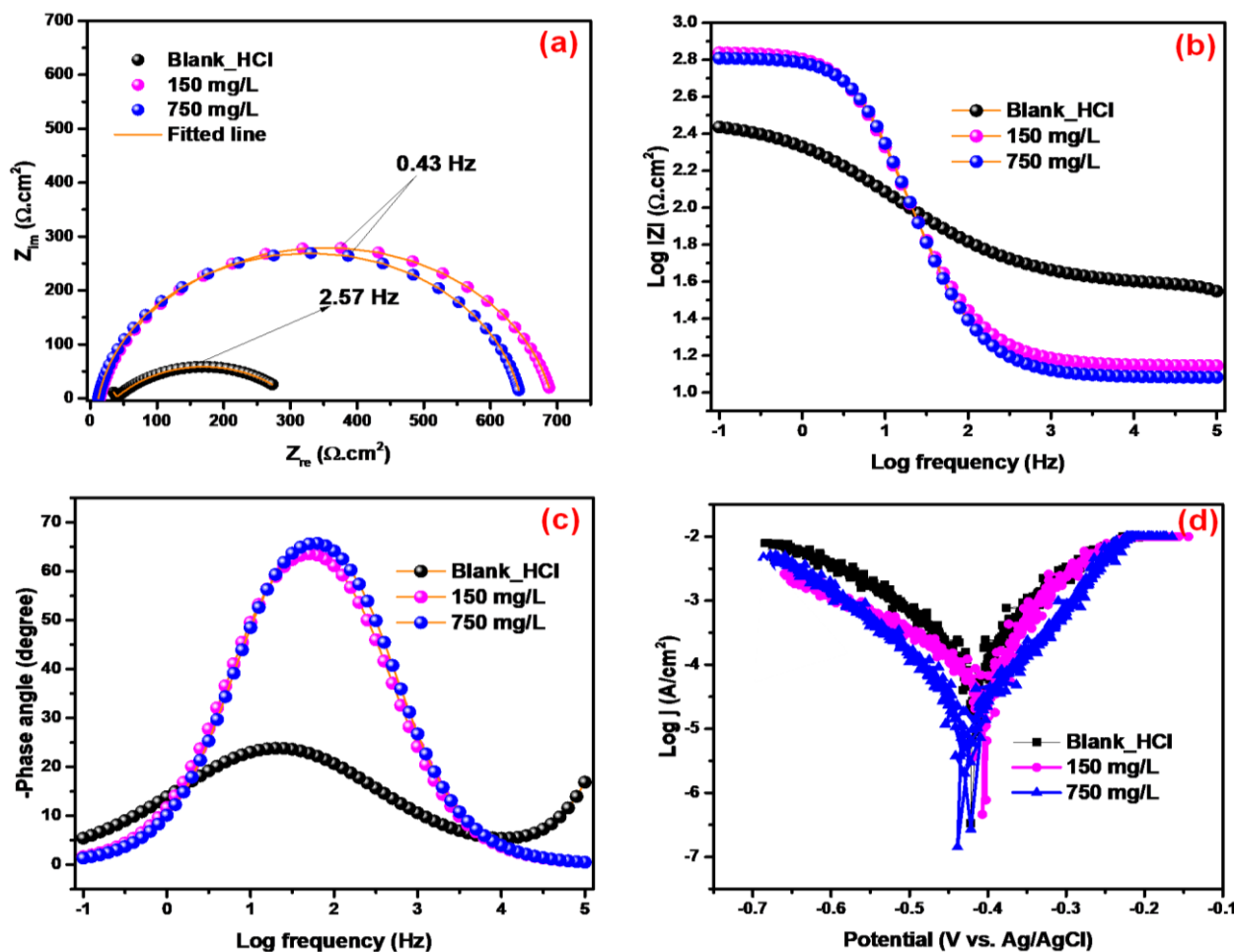


Figure 5. Electrochemical impedance spectra and potentiodynamic polarization curves for low carbon steel in 0.5 M HCl at room temperature; (a) Nyquist impedance plots (b) Bode plots (c) Phase-angle plots, and (d) Tafel anodic and cathodic polarization curves

Table 3. EIS fitting data for corrosion of low carbon steel in 0.5 M HCl solution without and with different concentrations of DDL-based inhibitor extract at room temperature

$C_{inh.}$ (mg/L)	R_s ($\Omega \cdot cm^2$)	CPE_1		R_{po} ($\Omega \cdot cm^2$)	CPE_2		R_{ct} ($\Omega \cdot cm^2$)	X^2 (10^{-1})	η_{EIS} (%)
		$Y_{01}(x10^{-8})$ ($\Omega^{-1} cm^{-2}$)	n_1		$Y_{02}(x10^{-8})$ ($\Omega^{-1} cm^{-2}$)	n_2			
Blank	0.01	1.17	0.80	25.82± 0.01	0.79	0.90	264.20± 0.05	1.13	-
150	0.03	0.11	0.91	26.32± 0.13	0.77	0.97	673.68± 0.66	1.11	60.78
750	0.01	0.21	0.87	24.22± 0.11	0.78	0.88	625.78± 0.65	1.15	57.78

The slight depreciation in the diameter of the Nyquist semicircle on addition of 750 mg/L DDL extract agrees with the slight decline in the inhibitor efficiency at that extract dosage as observed in the experiments with H_2SO_4 environment. This observation reveals that 750 mg/L of the extract exceeded the optimum concentration of the DDL extract necessary for the saturation of the adsorbed inhibitor film on the substrate surface as similar trend has been reported by Ofuyekpone *et al.* (2021) and other

research scholars (Eddy *et al.*, 2010; Al-Mhyawi, 2014; Ihebrodike *et al.*, 2010; Li *et al.*, 2019). This further shows that DDL-based inhibitor apparently exhibited similar inhibitory attitude towards dissolution of low-carbon steel in H₂SO₄ and HCl environments.

Figure 5d shows the Tafel polarization curves of low carbon steel after 30 minutes of immersion in 0.5 M HCl solution without and with different concentrations of DDL-based inhibitor at room temperature. The electrochemical parameters of the potentiodynamic polarization measurements such as the corrosion potential (E_{corr}), the corrosion current density (I_{corr}), the anodic (β_a) and cathodic (β_c) Tafel slopes, the inhibitor efficiency ($\eta\%$) and the degree of surface coverage (θ) after 30 minutes immersion are presented in Table 4.

Table 4. Potentiodynamic polarization parameters recorded for low carbon steel corroding in 0.5 M HCl without and with different concentrations of DDL-based inhibitor at room temperature

C_{inh} (mg/L)	E_{corr} (mV vs. Ag/AgCl)	I_{corr} (mA cm ⁻²)	β_a (mV dec ⁻¹)	β_c (mV dec ⁻¹)	$\eta\%$	θ
Blank	-390.57 ± 2.11	885.06 ± 1.11	109.20	86.11	-	-
150	-400.57 ± 1.08	301.75 ± 1.02	96.33	98.30	65.91	0.66
750	-440.61 ± 1.07	361.49 ± 0.18	88.61	64.33	59.16	0.59

The Tafel plots in Figure 5d reveals that increasing the dosage of the DDL-based inhibitor significantly affected the polarization parameters, displacing the corrosion potentials to the more passive region upon addition of the inhibitor. This shift in potential suggests improved preservation of the low-carbon steel from the attack of the hostile acid solution. Reports available in the literature have indicated that a corrosion inhibitor is a mixed-type inhibitor if the recorded change in corrosion potential is <85 mV while values of corrosion potential >85 mV suggests either anodic or cathodic type inhibitor (Ofuyekpone *et al.*, 2021). The highest shift (change) in the corrosion potential recorded in this experiment was 50.04 mV, hence a mixed-type behavior was indicated. Reports have shown that corrosion rate is directly proportional to the corrosion current density (Ofuyekpone *et al.*, 2021). The values of corrosion current density in Table 4 tremendously depreciated from 885.06 mA cm⁻² in the uninhibited acid environment to 301.75 mA cm⁻² on addition of 150 mg/L of the DDL-extract, suggesting reduced corrosion rate. Inhibitor efficiency of 65.91% was recorded relative to the uninhibited medium. This trend underscores the potency and ability of the DDL-extract to suppress the corrosion reaction in the HCl solution. The inhibitor efficiency was calculated from the polarization data according to Oguzie *et al.* (2007) using the expression in Equation 6.

3.4 Findings from Electrochemical Experiments with 0.5 M HNO₃ Solution

The data from electrochemical impedance spectroscopy and potentiodynamic polarization evaluated for low carbon steel/electrolyte interface without and with different concentrations of DDL-based inhibitor in 0.5 M HNO₃ solution at room temperature are shown as spectra in Figure 6.

Figure 6, panels a, b and c indicate the electrochemical impedance data presented as impedance spectra which, respectively, represent the Nyquist impedance plots, Bode plots and Phase-angle plots recorded for low carbon steel corroding in 0.5 M HNO₃ solution without and with different concentrations of DDL-based inhibitor. After 1800 s of free immersion in the 0.5 M HNO₃ solution without and with the inhibitor, it could be noticed that the low-carbon steel also attained a stable open circuit potential as revealed in Figure 4.

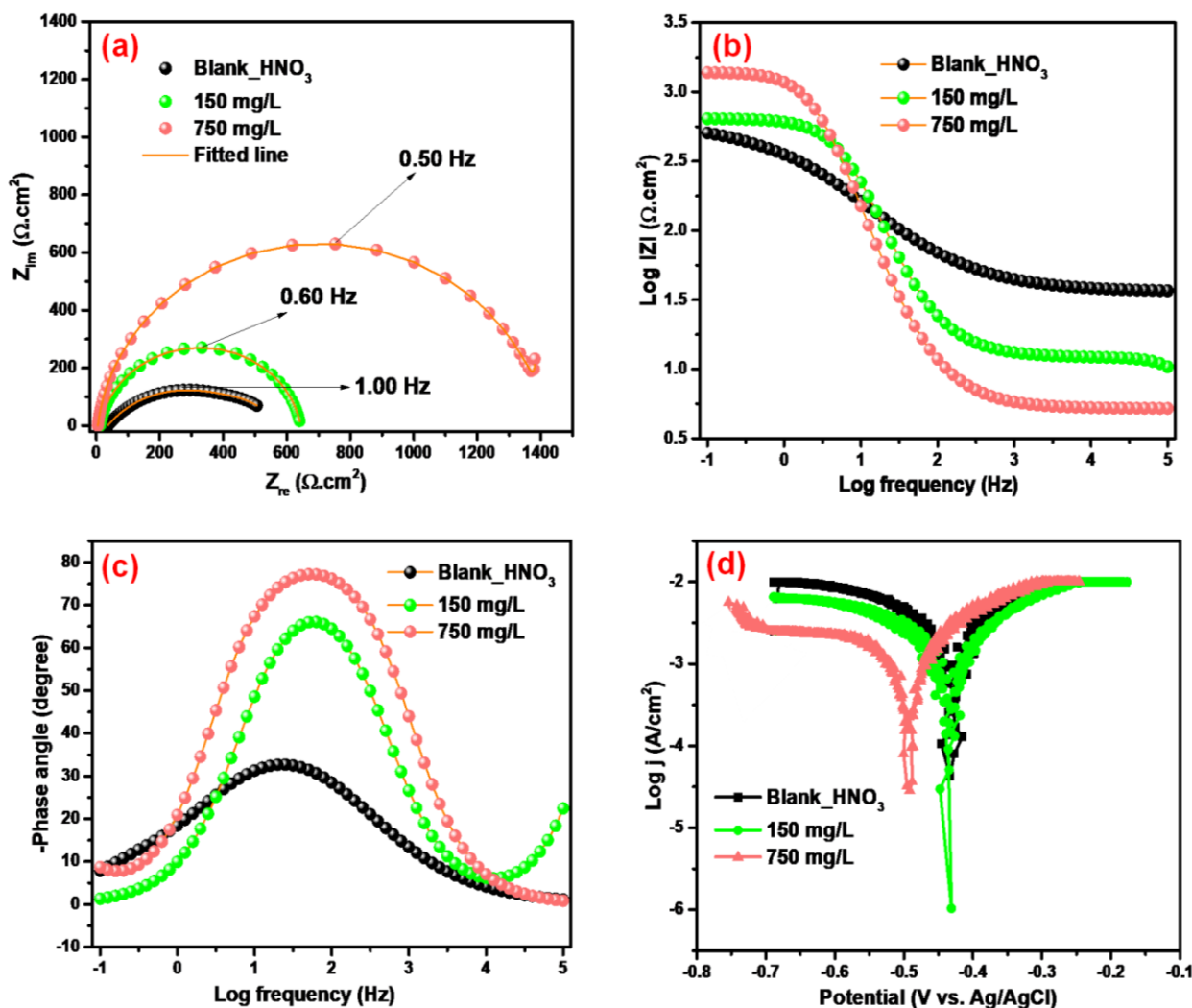


Figure 6. Electrochemical impedance spectra and potentiodynamic polarization curves for low carbon steel in 0.5 M HNO₃ at room temperature; (a) Nyquist impedance plots (b) Bode plots (c) Phase-angle plots, and (d) Tafel anodic and cathodic polarization curves

The Nyquist plots (Figure 6a) obtained at every extract concentration again displayed identical semicircles but different sizes whose diameters increase with higher extract concentration. The Nyquist semicircles got enlarged maximally upon addition of 750 mg/L of the extract, producing inhibitor protection efficacy of 72.43 % relative to the blank or uninhibited environment. This was accompanied with a corresponding increase in impedance of the interface as seen in the Bode plots in Figure 6b, and also in the maximum phase-angle in Figure 6c. The enlargement of the Nyquist semicircles makes it evident that corrosion resistance was impacted on the low-carbon steel coupons by the DDL extract and the resistance got improved with increasing extract concentration. This phenomenon is commonly associated with metal-electrolyte interaction caused by the roughness and inhomogeneity of the electrode surface (Fawcett *et al.*, 1992; Solomon *et al.*, 2010; Lebrini *et al.*, 2007). The values of the electrochemical fitting parameters deduced from the Nyquist plots are given in Table 5. With a cursory look at the data in the data in Table 5, it can be seen that the values of the charge transfer resistance (R_{ct}) are directly proportional to the concentration of the DDL-extract. The R_{ct} increased from 397.32 $\Omega \cdot cm^2$ in the uninhibited environment (blank) to 1441.04 $\Omega \cdot cm^2$ at 750 mg/L of DDL-extract, with a corresponding increase in inhibitor efficiency to 72.43 % relative to the blank medium. The inhibitor efficiency was calculated from the experimental data according to Oguzie *et al.* (2007) using the

expression in Equation 5 and the fitting of the electrochemical impedance spectrum for the Nyquist plots to an equivalent circuit model (ECM) is the same as that shown in Figure 4.

Table 5. EIS fitting data for corrosion of low carbon steel in 0.5 M HNO₃ solution without and with different concentrations of DDL-based inhibitor extract at room temperature

C_{inh} (mg/L)	R_s ($\Omega \cdot cm^2$)	CPE_1		R_{po} ($\Omega \cdot cm^2$)	CPE_2		R_{ct} ($\Omega \cdot cm^2$)	X^2 (10^{-1})	η_{EIS} (%)
		$(x10^{-8})Y_{01}$ ($\Omega^{-1} cm^{-2}$)	n_1		$(x10^{-8})Y_{02}$ ($\Omega^{-1} cm^{-2}$)	n_2			
Blank	0.01	0.41	0.80	52.68 ± 0.01	0.12	0.90	397.32 ± 0.11	1.33	-
150	0.01	0.29	0.91	12.17 ± 0.13	1.62	0.97	617.83 ± 0.63	1.15	35.69
750	0.01	0.50	0.89	8.96 ± 0.11	0.14	0.89	1441.04 ± 0.45	1.11	72.43

Comparing the data in Table 5 with those in Tables 1 and 3, and comparing Figure 6 with Figures 3 and 5 shows that low-carbon steel surface requires more than 750 mg/L of DDL-inhibitor to reach saturation point with the adsorbed inhibitor film when freely immersed in HCl hostile solution. The implication of this observation is that DDL-extract is not as potent in HNO₃ medium as it is in H₂SO₄ and HCl media. This result or trend is very consistent with what was recorded in the gravimetric (mass loss) approach. Figure 6d shows the potentiodynamic polarization curves of low carbon steel after 30 minutes of immersion in 0.5 M HNO₃ solution without and with different concentrations of DDL-based inhibitor at room temperature. The electrochemical parameters of the potentiodynamic polarization measurements such as the corrosion potential (E_{corr}), the corrosion current density (I_{corr}), the anodic (β_a) and cathodic (β_c) Tafel slopes, the inhibitor efficiency ($\eta\%$) and the degree of surface coverage (θ) after 30 minutes immersion are presented in Table 6.

Table 6. Potentiodynamic polarization parameters recorded for low carbon steel corroding in 0.5 M HNO₃ without and with different concentrations of DDL-based inhibitor at room temperature

C_{inh} (mg/L)	E_{corr} (mV vs. Ag/AgCl)	I_{corr} (mA cm ⁻²)	β_a (mV dec ⁻¹)	β_c (mV dec ⁻¹)	$\eta\%$	θ
Blank	-420.57 ± 2.11	869.06 ± 1.11	154.55	98.12	-	-
150	-430.57 ± 1.08	571.75 ± 1.11	88.13	86.54	34.21	0.34
750	-480.61 ± 1.07	301.49 ± 0.19	68.84	67.71	65.31	0.65

The Tafel plots in Figure 6d reveals that increasing the dosage of the DDL-based inhibitor significantly affected the polarization parameters, displacing the corrosion potentials to the more passive region upon addition of the inhibitor. This shift in potential suggests improved preservation of the low-carbon steel from the attack of the hostile acid solution. It has been previously reported that a corrosion inhibitor is a mixed-type inhibitor if the recorded change in corrosion potential is <85 mV while values of corrosion potential > 85 mV suggests either anodic or cathodic type inhibitor (Ofuyekpone *et al.*, 2021). The highest shift (change) in the corrosion potential recorded in this experiment was 60.04 mV, hence a mixed-type behavior was indicated. Reports (Ofuyekpone *et al.*, 2021; Arrousse *et al.*, 2020; Oguzie *et al.*, 2007) have also shown that corrosion rate is directly proportional to the corrosion current density. The values of corrosion current density in Table 6 significantly depreciated from 869.06 mA.cm⁻² in the uninhibited acid environment to 571.75 mA.cm⁻² on addition of 150 mg/L of the DDL-extract and further declined to 301.49 mA.cm⁻² when the DDL-

extract concentration was increased to 750 mg/L. This suggests reduced corrosion rate. Inhibitor efficiency of 65.31 % was recorded at the maximum inhibitor concentration relative to the uninhibited medium. This trend affirms the potency and ability of the DDL-extract to suppress the corrosion of low-carbon steel in the HNO₃ solution. The inhibitor efficiency was calculated from the polarization data according to [Oguzie et al. \(2007\)](#) using the expression in Equation 6.

These findings on efficiency obtained: H₂SO₄ > HCl > HNO₃ varied along the order of the corrosiveness of the acids, implying that the inhibitor is a very potent and sustainable one. The observed trend in agreement with the known literature that the corrosiveness of an acid or base is related to how severely it destroys surfaces and living tissues when brought in contact with such substrates. Both H₂SO₄ and HNO₃ are stronger acids and are more oxidizing and corrosive in nature than HCl solution. However, due to the existence of the a large amount of highly active Cl⁻ ions in HCl solution, the acid can destroy the passive protective film on the surface of metal substrates ([Fan et al., 2021](#)). Besides, equal molarity (0.5 M) of H₂SO₄, HCl and HNO₃ have pH values of 0.58, 0.301 and 0.30 respectively. These could be an explanation to the observed trend between HCl and HNO₃.

Conclusions

From the results, the following conclusions can be drawn.

1. *Datura discolor* Bernh. crude leaf extract effectively suppressed the corrosion of low-carbon steel in solutions of H₂SO₄, HCl and HNO₃.
2. The inhibitory effect of the extract is due to the presence of organic molecules contained in the leaf extract as reported by previous researchers and these organic molecules contain critical functional groups that function as active sites for inhibitor adsorption.
3. For a 150 mg/L dosage of the inhibitor in different electrolytes, efficacy of the inhibitor and the stability of its adsorbed passive film decreased in the order; Electrochemical impedance spectroscopy: H₂SO₄ > HCl > HNO₃ and Potentiodynamic polarization: H₂SO₄ > HCl > HNO₃, implying that the inhibitor exhibited best efficacy in H₂SO₄ and least in HNO₃ solution.
4. Both H₂SO₄ and HCl solutions have been reported to exhibit very similar model parameters for charge transfer reactions which manifests in comparable influence on the efficiency of corrosion inhibitors in equal concentration of electrolytes (Agarwal & Landolt, 1998). These scholars developed a theoretical model that was able to describe the observed influence of the nature and concentration of electrolyte anions and the inhibitors on the rate of anodic dissolution of the substrate. The result of the modelling revealed that both H₂SO₄ and HCl have very similar model parameters for charge transfer reactions which was evident in the equal anodic and cathodic Tafel slopes of dissolution.

Acknowledgements: The Principal Researcher (Cornelius Ahanotu) wishes to gratefully acknowledge the funding granted by the Tertiary Education Trust Fund (TETFund), Nigeria for carrying out the research through the Academic Staff Training and Development (AST&D) Interventions. He is also immensely grateful to Centre for Oilfield Chemical Research (CEFOR), University of Port Harcourt, Nigeria, for providing the equipment used for the electrochemical experiments.

Disclosure statement: *Conflict of Interest:* The authors declare that there are no conflicts of interest.

Compliance with Ethical Standards: This article does not contain any studies involving human or animal subjects.

References

- Abboud Y., Abourriche A., Tanane O., Hammouti B., Saffaj T., Ainane T., Berrada M., Charrouf M., Bennamara A. (2009), Corrosion inhibition of carbon steel in acidic media by *Bifurcaria bifurcata* extract, *Chem. Eng. Comm.* 196 N°7, 788-800.
- Agarwal, P. & Landolt, D. (1998). Effect of anions on the efficiency of aromatic carboxylic acid corrosion inhibitors in near neutral media: experimental investigation and theoretical modeling. *Corr. Sci.*, 40(415): 673-69
- Ahanotu, C.C., Onyeachu, I.B., Solomon, M.M., Chikwe, I.S., Chikwe, O.B., Eziukwu, C.A. (2020). *Pterocarpus santalinoides* leaves extract as a sustainable and potent inhibitor for low carbon steel in a simulated pickling medium, *Sustainable Chemistry and Pharmacy*, 15, 100196. DOI: [10.1016/j.scp.2019.100196](https://doi.org/10.1016/j.scp.2019.100196)
- Ahanotu, C.C., Madu, K.C., Chikwe, I.S. & Chikwe, O.B. (2022). The inhibition behaviour of extracts from *Plumeria rubra* on the corrosion of low carbon steel in sulphuric acid solution. *J. Mater. Environ. Sci.*, 13(09), 1025-1036
- Al-Mhyawi, S.R. (2014). Inhibition of mild steel corrosion using Junepurus plants as green inhibitor. *Afr. J. Pure Appl. Chem.*, 8(1), 9–22
- Al-Moghrabi, R.S., Abdel-Gaber, A.M., & Rahal, H.T. (2019). Corrosion inhibition of Mild Steel in Hydrochloric and Nitric Acid Solutions Using Willow Leaf Extract. *Protection of Metals and Physical Chemistry of Surfaces*, 55(3), 603–607
- Arrousse, N., Salim, R., Houari, G.A. *et al.* (2020) Experimental and theoretical insights on the adsorption and inhibition mechanism of (2E)-2-(acetylamino)-3-(4-nitrophenyl) prop-2-enoic acid and 4-nitrobenzaldehyde on mild steel corrosion. *J. Chem. Sci.* 132, 112. <https://doi.org/10.1007/s12039-020-01818-w>
- Dafali A., Hammouti B., Touzani R., *et al.* (2002), Corrosion Inhibition of copper in 3% NaCl solution by new bipyrazolic derivatives, *Anti-corros. Meth. & Mat.*, 49N°2, 96-104.
- da Rocha, J.C., da Cunha Ponciano Gomes, J.A. and D'Elia, E. (2010). Corrosion inhibition of carbon steel in hydrochloric acid solution by fruit peel extract *Corrosion Science*, 52, 2341-2348.
- Deng, S. & Li, X. (2012). Inhibition by *Ginkgo* leaves extract of the corrosion of steel in HCl and H₂SO₄ solutions. *Corr. Sci.*, 55, 407–415
- Diass K., Merzouki M., El Fazazi K., *et al.* (2023). Essential oil of *Lavandula officinalis*: Chemical composition and antibacterial activities, *Plants*, 12, 1571. doi.org/10.3390/plants12071571
- Ebenso, E.E., Eddy, N.O. & Odiongenyi, A.O. (2008). Corrosion inhibitive properties and adsorption behavior of ethanol extract of *Piper guineense* as a green corrosion inhibitor for mild steel in H₂SO₄. *African Journal of Pure and Applied Chemistry*, 2(11), 107-115
- Eddy, N.O. & Ebenso, E.E. (2008). Adsorption and inhibitive properties of ethanol extracts of *Musa sapientum* peels as a green corrosion inhibitor for mild steel in acidic medium. *Afr. J. Pure Appl. Chem.* 2 (6), 046 – 054
- Eddy, N.O., Awe, F. & Ebenso, E.E. (2010). Adsorption and inhibitive properties of ethanol extract of leaves of *Solanum melongena* for the corrosion of mild steel in 0.1M HCl. *Int. J. Electrochem. Sci.*, 5, 1996–2011
- El Ouafi A., Hammouti B., Oudda H., Kertit S., Touzani R., Ramdani A. (2002), New bipyrazole derivatives as effective inhibitors for the corrosion of mild steel in 1M HCl medium, *Anti-Corrosion Methods and Materials*, 49, 199-204.
- Fan, R., Zhang, W., Wang, Y., Chen, D. & Zhang, Y. (2021). Metal Material Resistant to Hydrochloric Acid Corrosion. *J. Phys.: Conf. Ser.* 1732 012134

- Fawcett, W.R., Kovacova, Z., Motheo, A.J. & Foss, C.A. (1992). Application of the AC admittance technique to double-layer studies on polycrystalline gold electrodes. *J. Electroanal. Chem.*, 326(1-2), 91-103
- Haddou S., Mounime K., Loukili E. H., *et al.* (2023) Investigating the Biological Activities of Moroccan Cannabis Sativa L Seed Extracts: Antimicrobial, Anti-inflammatory, and Antioxidant Effects with Molecular Docking Analysis, *Mor. J. Chem.*, 11(4), 1116-1136
- Hmamou B.D., Salghi R., Zarrouk A., *et al.* (2012) Inhibition of steel corrosion in hydrochloric acid solution by chamomile extract, *Der Pharma Chim.* 4 N°4, 1496-1505
- Hmamou D. B., Salghi R., Zarrouk A., *et al.* (2015), Investigation of corrosion inhibition of carbon steel in 0.5 M H₂SO₄ by new bipyrazole derivative using experimental and theoretical approaches, *Journal of Environmental Chemical Engineering*, 3 N°3, 2031-2041
- Hossain, N., Chowdhury, M.A., Rana, M. *et al* (2022). Terminalia arjuna leaves extract as green corrosion inhibitor for mild steel in HCl solution. *Result Eng.* 14, 100438
- Ihebroke, M.M., Uroh, A.A. & Okeoma, B.K. (2010). The inhibitive effect of *Solanum melongena* L. Leaves extract on the corrosion of Aluminum in H₂SO₄ acid. *Afr. J. Pure Appl. Chem.*, 4(8), 158–165
- Ji, G., Shukla, S.K., Ebenso, E.E. & Prakash, R. (2013). *Argemone mexicana* Leaf Extract for Inhibition of Mild Steel Corrosion in Sulfuric Acid Solutions. *Int. J. Electrochem. Sci.*, 8, 10878 – 10889
- Kasiri, M.B. & Safapour, S. (2014). Natural dyes and antimicrobials for green treatment of textiles. *Environ. Chem. Lett.*, 12, 1–13, [DOI 10.1007/s10311-013-0426-2](https://doi.org/10.1007/s10311-013-0426-2)
- Khadom, A.A. (2015) Kinetics and synergistic effect of iodide ion and naphthylamine for the inhibition of corrosion reaction of mild steel in hydrochloric acid. *Reac. Kinet. Mech. Cat.* 115, 463–481. <https://doi.org/10.1007/s11144-015-0873-9>
- Kissi, M, Bouklah, M, Hammouti, B. and Benkaddour, M. (2006). Establishment of equivalent circuits from electrochemical impedance spectroscopy study of corrosion inhibition of steel by pyrazine in sulphuric acidic solutions. *Applied Surface Science*, 252, 4190-4197
- Larabi, L., Harek, Y., Benali, O., Ghalem, S. (2005). Erratum to hydrazide derivatives as corrosion inhibitors for mild steel in 1 M HCl. *Prog. Org. Coat.* 54, 256-262
- Lebrini, M., Lagrenee, M., Vezin, H., Triasnel, M., Bentiss, F. (2007). Experimental and theoretical study for corrosion inhibition of mild steel in normal hydrochloric acid solution by some new macrocyclic polyether compounds. *Corr. Sci.*, 49, 2254-2269
- Li, D., Panpan, Z., Xinyu, G. *et al* (2019). The inhibition of mild steel corrosion in 0.5M H₂SO₄ solution by radish leaf extract. *RSC Adv.* 9, 40997. <https://doi.org/10.1039/c9ra04218k>
- Mihit M., Salghi R., El Issami S., *et al.* (2006), A study of tetrazoles derivatives as corrosion inhibitors of copper in nitric acid, *Pigm. Resin Technol.* 35 N° 3, 151-157. <https://doi.org/10.1108/03699420610665184>
- Ofuyekpone O.D., Utu O.G., Onyekpe B.O. & Adediran A.A. (2021). Effect of inhibitor concentration on the potency of *Stylosanthes gracilis* extract as corrosion inhibitor for AISI 3041 in sulphuric acid solution. *Scientific African*, 11, e00714, <https://doi.org/10.1016/j.sciaf.2021.e00714>
- Oguzie, E.E. (2005). Inhibition of acid corrosion of mild steel by *Telfaria occidentalis* extract, *Pigment & Resin Technol.* 34: 321 – 326
- Oguzie E.E., Onuoha G.N., Onuchukwu A.I. (2005) Inhibitory mechanism of mild steel corrosion in 2 M sulphuric acid solution by methylene blue dye. *Materials Chemistry and Physics*, 89, 305-311
- Oguzie E.E. (2006). Studies on the inhibition effect of *Occinum viridis* extract on acid corrosion of mild steel. *Mater. Chem. & Phys.* 99: 441- 446

- Oguzie, E.E., Li, Y. & Wang, E.H. (2007). Corrosion inhibition and adsorption behaviour of methionine on mild steel in sulfuric acid and synergistic effect of iodide ions. *J. Colloid. Interf. Sci.*, 310, 90-98
- Okafor, P.C., Ebenso, E.E. & Ekpe, U.J. (2010). *Azadirachta indica* extracts as corrosion inhibitor for mild steel in acid medium, *International Journal Electrochemical Science*, 5, 978-993
- Palumbo G., Swiech D., Górny M. (2023). Guar Gum as an Eco-Friendly Corrosion Inhibitor for N80 Carbon Steel under Sweet Environment in Saline Solution: Electrochemical, Surface, and Spectroscopic Studies. *Int. J. Mol. Sci.*, 24, 12269. <https://doi.org/10.3390/ijms241512269>
- Popova, A., Sokolova, E., Raicheva, S. & Christov, M. (2003). AC and DC study of the temperature effect on mild steel corrosion in acid media in the presence of benzimidazole derivatives. *Corros. Sci.*, 45, 33-38, [https://dx.doi.org/10.1016/S0010-938X\(02\)00072-0](https://dx.doi.org/10.1016/S0010-938X(02)00072-0)
- Puspitasari, P., Andoko, A., Suryanto, H., Risdanareni, P. & Yudha, S. (2017). Hardness improvement on low carbon steel using pack carbonitriding method with holding time variation. *MATEC Web of Conferences*, 01012, DOI: [10.1051/matecconf/201710101012](https://doi.org/10.1051/matecconf/201710101012)
- Raja, P. B., & Sethuraman, M.G. (2009). *Solanum tuberosum* as an inhibitor of mild steel corrosion in acid media. *Iranian Journal of Chemistry and Chemical Engineering*, 28 (1), 77-84
- Satapathy A.K., Gunasekaran G., Sahoo *et al.* (2009). Corrosion inhibition by *Justicia gendarussa* plant extract in hydrochloric acid solution. *Corrosion Science*, 51 (12), 2848-2856
- Sayed, S.Y., El-Deab M.S., El-Anadouli B.E. & Ateya B.G. (2003) Synergistic effects of benzotriazole and copper ions on the electrochemical impedance spectroscopy and corrosion behavior of iron in sulfuric acid. *J. Phys. Chem. B*, 107(23), 5575-5585
- Solomon, M.M, Umoren, S.A., Udosoro, I.I. & Udoh, A.P. (2010). Inhibitive and adsorptive behavior of carboxymethyl cellulose on mild steel corrosion in sulphuric acid solution. *Corros. Sci.*, 52(4): 1317-1325, doi: [10.1016/j.corsci.2009.11.041](https://doi.org/10.1016/j.corsci.2009.11.041)
- Umoren S.A., Li, Y. & Wang, F.H. (2011). Influence of iron microstructure on the performance of polyacrylic acid as corrosion inhibitor in sulfuric acid solution. *Corros. Sci.*, 53(5), 1778-1785
- Wang, K., Wang, B., Ma, H., Wang, Z., Liu, Y., Wang, Q. (2023). Natural Products for Pesticides Discovery: Structural Diversity Derivation and Biological Activities of Naphthoquinones Plumbagin and Juglone. *Molecules*, 28, 3328. <https://doi.org/10.3390/molecules28083328>

(2024) ; <http://www.jmaterenvironsci.com>